Electronic Supplementary Material (ESI) for Energy & Environmental Science.

Ternary nonfullerene polymer solar cells with efficiency >13.7% by integrating the advantages of materials and two binary cells

Xiaoling Ma,[a] Wei Gao,[b,d] Jiangsheng Yu,[c] Qiaoshi An,[a] Miao Zhang,[a] Zhenghao Hu,[a] Jianxiao Wang,[a] Weihua Tang,*[c] Chuluo Yang,*[b,d] and Fujun Zhang*[a]

a. Key Laboratory of Luminescence and Optical Information, Ministry of Education, Beijing Jiaotong University, Beijing 100044, China. E-mail: fjzhang@bjtu.edu.cn

b. College of Materials Science and Engineering, Shenzhen University, Shenzhen, 518060, China. E-mail: clyang@whu.edu.cn

c. Key Laboratory of Soft Chemistry and Functional Materials, Ministry of Education, Nanjing University of Science and Technology, Nanjing 210094, China. E-mail: whtang@njust.edu.cn

d. Hubei Collaborative Innovation Center for Advanced Organic Chemical Materials, Hubei Key Lab on Organic and Polymeric Optoelectronic Materials, Department of Chemistry, Wuhan University, Wuhan 430072, China

Experimental details

The patterned indium tin oxide (ITO) coated glass substrates (15 Ω per square) were cleaned via sequential sonication in detergent, de-ionized and ethanol and then blow-dried by high-purity nitrogen. All pre-cleaned ITO substrates were treated by oxygen plasma for 1 minute to improve their work function and clearance. The Zinc oxide (ZnO) solution was spin coated on ITO substrates at 4000 rounds per minute (RPM) for 30 seconds and annealed at 200°C for 1 hour in atmospheric air. Then ITO substrates coated with ZnO layer were transferred into a high-purity nitrogen-filled glovebox. The polymer donor PBDB-T (purchased from Organtec Materials Inc.), nonfullerene acceptors INPIC-4F and MeIC1 (used as received) were dissolved in chlorobenzene (with 0.5 vol% diiodooctane) to prepare 18 mg/ml blend solutions. The proportions of INPIC-4F:MeIC1 are 1:0, 0.9:0.1, 0.7:0.3, 0.5:0.5, 0.3:0.7, 0:1 and the weight ratio of donor to acceptor is kept constant as 1:1. The mixed solutions were spin-coated onto the ZnO/ITO substrates at 2600 RPM for 40 s and annealed at 120 °C for 10 minutes to prepare the active layers. A thin molybdenum trioxide (MoO_3) layer (10 nm) and a silver (Ag) layer (100 nm) were sequentially deposited by thermal evaporation. The active area is approximate 3.8 mm^2, which is defined by the overlapping area of ITO anode and Ag cathode. The current density-voltage (*J-V*) curves of all the polymer solar cells (PSCs) were measured by a Keithley 2400 unit in high-purity nitrogen-filled glove box. The AM 1.5G irradiation was provided by an XES-40S2 (SAN-EI ELECTRIC Co., Ltd) solar simulator (AAA grade, 70×70 mm^2 photobeam size) with light intensity of 100 mW cm^{-2}. The external quantum efficiency (EQE) spectra of PSCs were measured by a Zolix Solar Cell Scan 100. The absorption spectra of films were measured with a Shimadzu UV-3101 PC spectrometer. Grazing incidence X-ray diffraction (GIXD) images were measured by a 5-circle Huber diffractometer at the Beijing Synchrotron Radiation Facility (BSRF). A bent triangle silicon crystal was used to select the X-rays of a wavelength of 1.54 Å. A grazing incidence angle of 0.4° was chosen to increase GIXD peak intensity for investigating the crystallinity and orientation that prevail throughout the active layers. Transmission electron microscopy (TEM) images of active layers were obtained by a JEOL JEM-1400 transmission electron microscope operated at 80 kV.

Table S1. Photovoltaic parameters of ternary PSCs with 50 wt% MeIC1 in acceptors based on 20 cells.

Cells	*Jsc* (mA cm^{-2})	*Voc* (V)	FF (%)	PCE (%)	Cells	*Jsc* (mA cm^{-2})	*Voc* (V)	FF (%)	PCE (%)
No.1	21.30	0.88	70.60	13.23	No.11	21.26	0.88	72.68	13.60
No.2	21.60	0.87	70.68	13.28	No.12	21.51	0.88	71.44	13.52
No.3	21.55	0.88	70.37	13.34	No.13	21.77	0.87	71.22	13.49
No.4	21.44	0.88	70.81	13.36	No.14	21.54	0.88	71.47	13.55
No.5	21.47	0.88	71.02	13.42	No.15	21.38	0.88	71.92	13.53
No.6	21.51	0.88	70.79	13.40	No.16	21.42	0.88	71.53	13.48
No.7	21.49	0.87	71.42	13.35	No.17	21.36	0.88	71.57	13.45
No.8	21.54	0.88	70.80	13.42	No.18	21.55	0.88	71.69	13.60
No.9	21.83	0.87	71.15	13.51	No.19	21.84	0.87	71.84	13.65
No.10	21.21	0.88	72.41	13.52	No.20	21.86	0.88	71.39	13.73

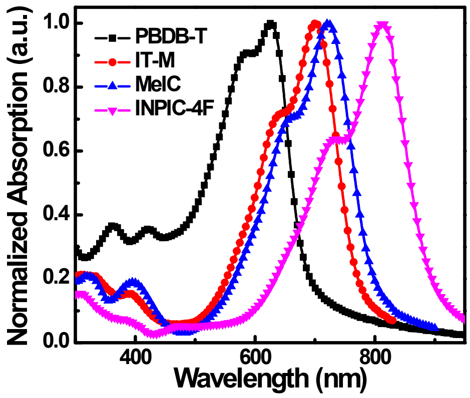

Fig. S1 Normalized absorption spectra of neat PBDB-T, IT-M, MeIC, INPIC-4F films.

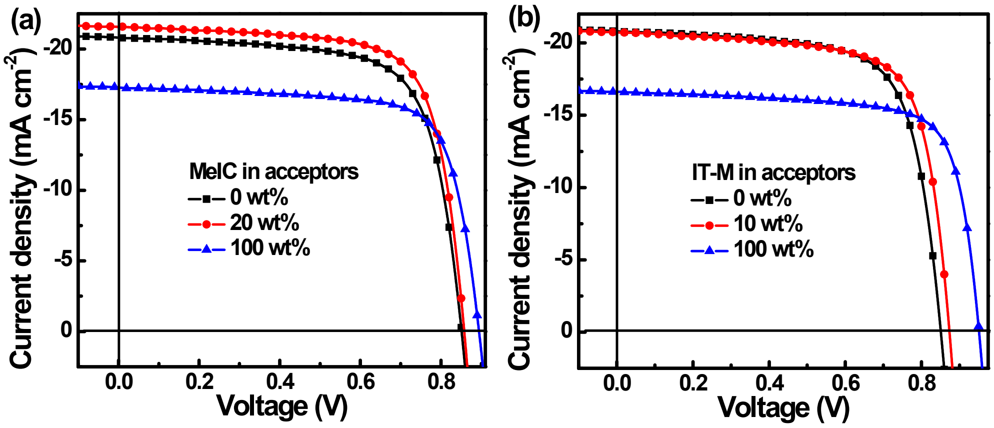

Fig. S2 *J-V* curves of the optimized binary and ternary PSCs with MeIC (a), IT-M (b) as the third component under AM 1.5G illumination with light intensity of 100 mW cm^{-2}.

Table S2 Photovoltaic parameters of the optimized binary and ternary PSCs with MeIC or IT-M as the third component.

The third component	Content (wt%)	J_{SC} (mA cm^{-2})	V_{OC} (V)	FF (%)	PCE (%)
MeIC	0	20.81	0.85	70.93	12.55
	20	21.57	0.86	72.20	13.40
	100	17.28	0.89	74.15	11.40
IT-M	0	20.81	0.85	70.93	12.55
	10	20.73	0.87	72.38	13.05
	100	16.62	0.95	74.83	11.82

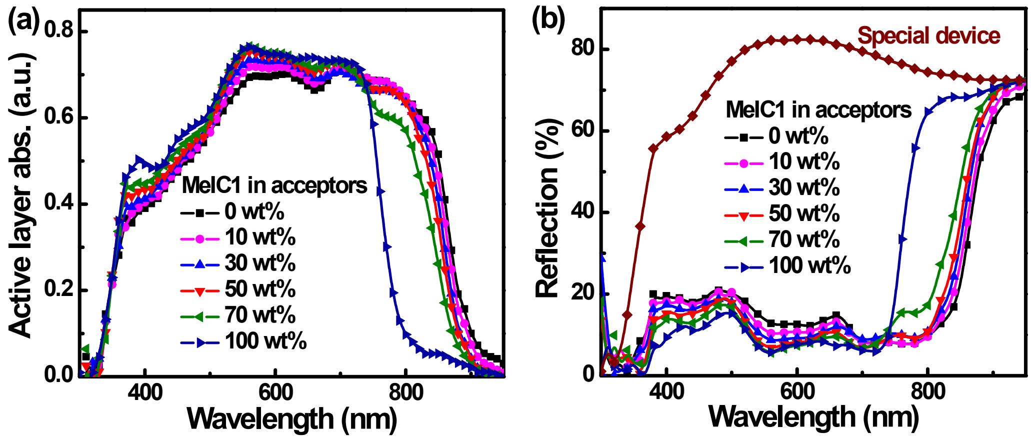

Fig. S3 (a) Absorption spectra of active layers with different MeIC1 content in cells. (b) The reflection spectra of all PSCs and a special device ITO/ZnO/PMMA (~120 nm)/MoO_3/Ag.

The reflection measurement of all devices was performed on a commercial QE measurement system (QE-RT3011, Enlitech) by using an integrating sphere. The absorption spectra of active layers were calculated by subtracting the parasitic absorptions (1-R_1) from the total absorption in PSCs (1-R_2), where R_1 is the reflection spectrum of device ITO/ZnO/PMMA (~120 nm)/MoO_3/Ag, R_2 is the reflection spectra of PSCs ITO/ZnO/active layers (~120 nm)/MoO_3/Ag. The 120 nm PMMA layer in the special cell is used to simulate the optical path in real PSCs because PMMA has negligible photon harvesting in the whole spectral range, and the light absorption of glass/ITO/ZnO layers in real PSCs can be obtained from this special cell.

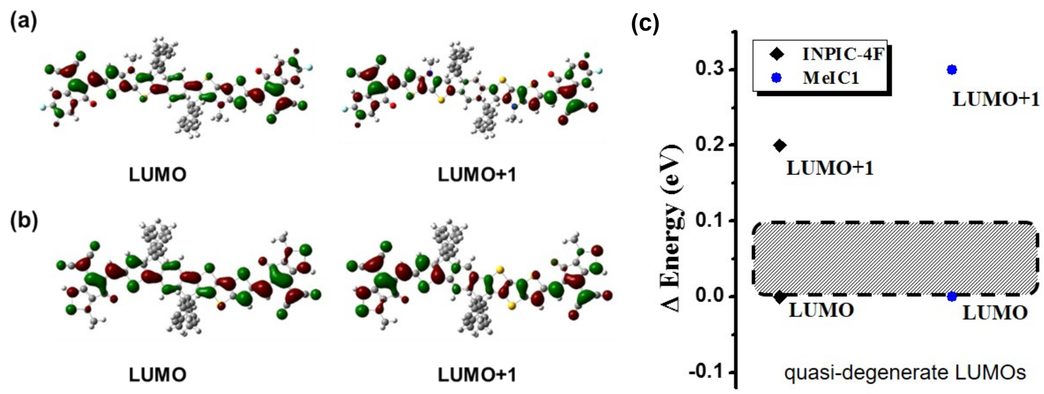

Fig. S4. Pictorial representations of the frontier molecular orbitals of INPIC-4F (a) and MeIC1 (b) from the DFT calculations. (c) Diagram of the frontier orbital energies of INPIC-4F and MeIC1.

Table S3 Summary of molecular weight, n, l, and N_e values of INPIC-4F and MeIC1.

Material	Molecular Weight (g mol^{-1})	n (mol g^{-1})	l	N_e (mol g^{-1})
INPIC-4F	1801	3.3×10^{20}	1	3.3×10^{20}
MeIC1	1467	4.1×10^{20}	1	4.1×10^{20}

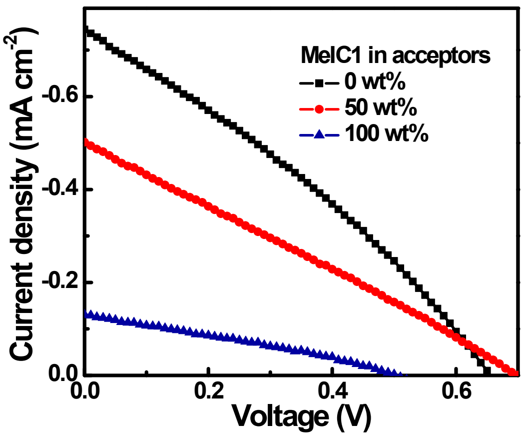

Fig. S5. J-V curves of the corresponding cells without PBDB-T.

Table S4. J_{ph}, J_{sat}, G_{max} and J_{ph}/J_{sat} values of typical PSCs.

MeIC1 content (wt %)	J_{ph}[a] (mA cm^{-2})	J_{ph}[b] (mA cm^{-2})	J_{sat} (mA cm^{-2})	G_{max} (m^{-3} s^{-1})	J_{ph}/J_{sat}[a] (%)	J_{ph}/J_{sat}[b] (%)
0	20.81	18.17	22.01	1.15×10^{28}	94.5	82.6
50	21.86	19.13	22.92	1.19×10^{28}	95.4	83.5
100	17.53	15.55	18.28	0.98×10^{28}	95.9	85.1

[a] short-circuit condition, [b] maximal power output condition.

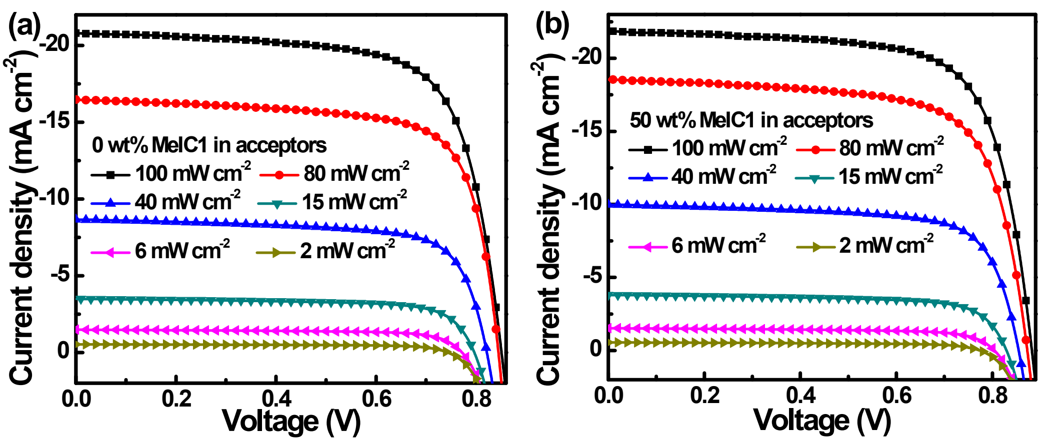

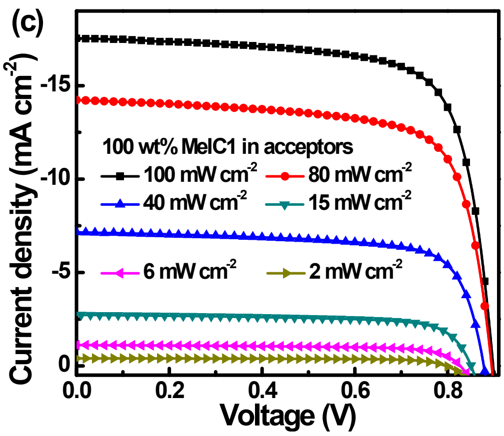

Fig. S6. The *J-V* curves of the PSCs with 0 wt% (a), 50 wt% (b), and 100 wt% (c) MeIC1 contents in acceptors under different light illumination intensity, obtained from standard AM 1.5G (100 mW cm^{-2}) illumination using a set of neutral optical filters.

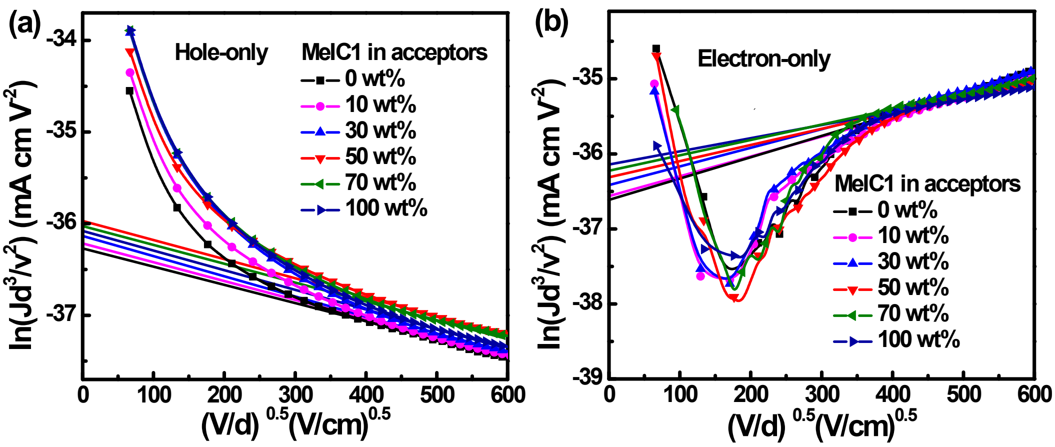

Fig. S7. The plotted ln(Jd^3/V^2) versus $(V/d)^{0.5}$ curves of the devices with different MeIC1 content.

Table S5. Hole and electron mobility in PSCs with different MeIC1 content.

MeIC1 content (wt %)	μ_h (cm^2 V^{-1} s^{-1})	μ_e (cm^2 V^{-1} s^{-1})	μ_h/μ_e
0	5.93×10^{-4}	4.22×10^{-4}	1.41
10	6.23×10^{-4}	4.48×10^{-4}	1.39
30	7.00×10^{-4}	5.15×10^{-4}	1.36
50	7.77×10^{-4}	5.75×10^{-4}	1.35
70	7.54×10^{-4}	6.17×10^{-4}	1.22
100	7.31×10^{-4}	6.62×10^{-4}	1.10

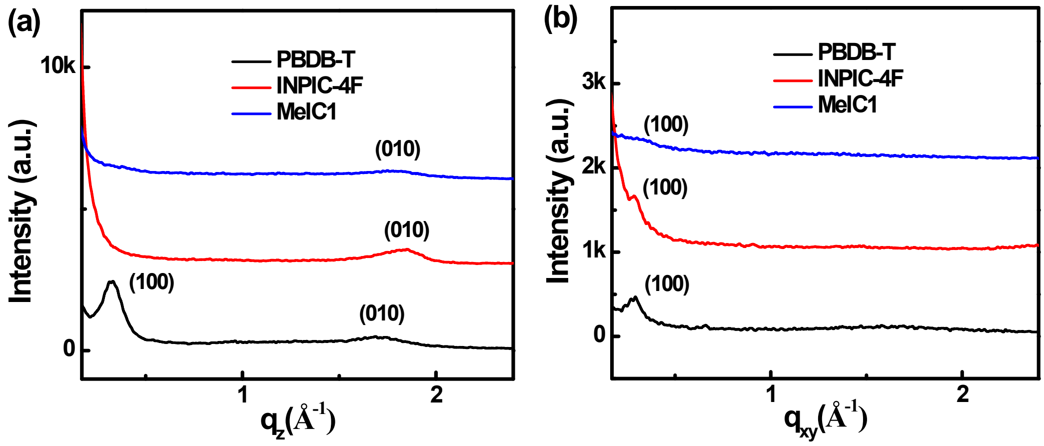

Fig. S8. Out-of-plane (a) and in-plane (b) GIXD profiles for the neat PBDB-T, INPIC-4F, and MeIC1 films.